

RESEARCH

Open Access



Intestinal commensal bacteria promote *Bactrocera dorsalis* larval development through the vitamin B6 synthesis pathway

Jian Gu¹, Zhichao Yao^{1,2}, Bruno Lemaitre³, Zhaohui Cai^{1,4*}, Hongyu Zhang^{1*} and Xiaoxue Li^{1*}

Abstract

Background The gut microbiota can facilitate host growth under nutrient-constrained conditions. However, whether this effect is limited to certain bacterial species remains largely unclear, and the relevant underlying mechanisms remain to be thoroughly investigated.

Results We found that the microbiota was required for *Bactrocera dorsalis* larval growth under poor dietary conditions. Monoassociation experiments revealed that *Enterobacteriaceae* and some *Lactobacilli* promoted larval growth. Among the 27 bacterial strains tested, 14 significantly promoted larval development, and the *Enterobacteriaceae cloacae* isolate exhibited the most obvious promoting effect. A bacterial genome-wide association study (GWAS) revealed that the vitamin B6 synthesis pathway was critical for the promotion of *E. cloacae* growth. Deletion of *pdxA*, which is responsible for vitamin B6 biosynthesis, deprived the mutant strains of larval growth-promoting function, indicating that the 4-hydroxythreonine-4-phosphate dehydrogenase (*pdxA*) gene was crucial for promoting larval growth in *E. cloacae*. Importantly, supplementation of a poor diet with vitamin B6 successfully rescued the axenic larval growth phenotype of *B. dorsalis*.

Conclusion Our results suggest that gut microbes promote insect larval growth by providing vitamin B6 under nutrient scarcity conditions in *B. dorsalis*.

Keywords *Bactrocera dorsalis*, Gut microbiota, Bacterial genome-wide association study, Vitamin B6, Nutrient deficiency

*Correspondence:

Zhaohui Cai
caizhh@tib.cas.cn
Hongyu Zhang
hongyu.zhang@mail.hzau.edu.cn
Xiaoxue Li
xiaoxueli@mail.hzau.edu.cn

¹ National Key Laboratory for Germplasm Innovation and Utilization for Fruit and Vegetable Horticultural Crops, Hubei Hongshan Laboratory, China-Australia Joint Research Centre for Horticultural and Urban Pests, Institute of Urban and Horticultural Entomology, College of Plant Science and Technology, Huazhong Agricultural University, Wuhan 430070, China

² College of Plant Protection, Yangzhou University, Yangzhou 225009, China

³ Global Health Institute, School of Life Science, École Polytechnique Fédérale de Lausanne (EPFL), Lausanne, Switzerland

⁴ Key Laboratory of Engineering Biology for Low-Carbon Manufacturing, Tianjin Institute of Industrial Biotechnology, Chinese Academy of Sciences, Tianjin 300308, China



© The Author(s) 2024. **Open Access** This article is licensed under a Creative Commons Attribution-NonCommercial-NoDerivatives 4.0 International License, which permits any non-commercial use, sharing, distribution and reproduction in any medium or format, as long as you give appropriate credit to the original author(s) and the source, provide a link to the Creative Commons licence, and indicate if you modified the licensed material. You do not have permission under this licence to share adapted material derived from this article or parts of it. The images or other third party material in this article are included in the article's Creative Commons licence, unless indicated otherwise in a credit line to the material. If material is not included in the article's Creative Commons licence and your intended use is not permitted by statutory regulation or exceeds the permitted use, you will need to obtain permission directly from the copyright holder. To view a copy of this licence, visit <http://creativecommons.org/licenses/by-nc-nd/4.0/>.

Introduction

Insects, like other animals, are closely associated with microorganisms. Microorganisms have strong effects on the physiological, ecological, and evolutionary functions of insects [1, 2]. Microorganisms, including bacteria, archaea, fungi, viruses, and others, may have enduring or transient interrelationships with their insect hosts, which may be beneficial or detrimental to insect health [1]. Although microorganisms may be pathogenic to insects, thus reducing host viability and increasing morbidity [3], commensal microorganisms within insects can be helpful or even essential for host survival.

Commensal microorganisms provide protection to the host against various stresses, such as temperature, drought, and heavy metal stresses, as well as biological stresses from nematodes, fungi, and parasites [4]. The greater wax moth *Galleria mellonella* can digest polyethylene with the aid of the intestinal microbiome [5]. The endosymbiont *Buchnera* increases the thermotolerance of its host aphid, and this effect is associated with the inclusion of body-associated protein A (*ibpA*) gene in aphids [6]. The bacterium *Hamiltonella defensa* can provide protection against parasitoids in pea aphids [7–11]. Another symbiont, *Regiella insecticola*, can offer protection against fungal infection and enhance resistance to parasitoids, thus promoting pea aphid survival [12, 13]. This protection is also common in other insects. The gut symbiotic bacterium *Burkholderia* increases the resistance of its host bean bug *Riptortus pedestris* to the pesticide fenitrothion [14]. In *Oryzaephilus surinamensis* insects, symbionts affect cuticle thickness, thus promoting desiccation resistance under dry conditions [15]. Two core microbes, *Snodgrassella alvi* and *Lactobacillus bombicola*, in bumble bees increase host survival when the host is exposed to selenate [16]. The bacterial communities in the eggs and larvae of chironomids play a role in protecting hosts from toxicants [17]. These findings illustrate the contribution of the microbiota to host fitness by supplementing host metabolic pathways or increasing the resistance of hosts to stresses [1].

Many insects live in nutrient-limited environments, which significantly impacts their physiological activity. Under these nutrient-constrained conditions, insect microbes can provide nutrients to their hosts. A case in point is that aphids live by sucking plant phloem sap, but the essential amino acid tryptophan is not present in phloem sap [18, 19], and this amino acid is supplied by the aphid's primary symbiotic bacterium, *Buchnera aphidicola* [20–23]. Another example is that the nutrient supply of the glassy-winged leafhopper *Homalodisca coagulata* is dependent on two symbiotic bacteria, *Baumannia cicadellincola* and *Sulcia muelleri*, of

which *B. cicadellincola* provides the host with vitamins and coenzymes, while *S. muelleri* provides some essential amino acids, thus ensuring the metabolic functions of the host [24]. In Hemiptera insects that feed on bast sap, the symbiotic bacterium *Sulcia* sp. has evolved a dual symbiotic relationship with the host and a variety of endosymbiotic bacteria, and the reduced genome of *Sulcia* sp. makes it dependent on other symbiotic bacteria to synthesize all essential amino acids [25, 26]. The symbiotic bacterium *Candidatus Erwinia dacicola* in the olive fruit fly *Bactrocera oleae* can extract nitrogen from environmental wastes such as bird droppings, thus providing adult flies with essential amino acids and increasing their reproductive capacity [27]. Many studies have highlighted the role of the microbiota in providing the host with choline, thiamine, and amino acids in the model organism *Drosophila melanogaster* [28–30]. Several studies have indicated that the presence of symbiotic bacteria promotes the growth of *Drosophila* larvae [31–33]. An integrated nutritional network established based on a systematic nutritional screening method revealed the complex interactions between the host *Drosophila* and its microbiota species [34].

Previous research has focused on the identification of a single microbiota species that alters host traits. However, insect microbiomes are often composed of various bacteria from different orders and families that work jointly to affect the host. Here, we analyzed the collective function of the gut microbiomes of the invasive horticultural pest *Bactrocera dorsalis* in altering or promoting host adaptability. *B. dorsalis* is a fruit fly that causes damage to over 350 different fruits and vegetables, and the microbiota in *B. dorsalis* plays multiple roles in the host's physiological processes, including cold adaptation, survival after irradiation, reproductive behaviour, and invasion [35–38].

In the present study, we investigated the role of the microbiota in larval development of *B. dorsalis*. Use of 16 s rRNA sequencing revealed that as larvae grew and developed, the richness and diversity of the gut microbial communities of *B. dorsalis* gradually decreased. The microbiota is required for fly growth under poor-nutrient dietary conditions. A monoassociation experiment indicated that, of 27 tested bacterial species, at least 14 promoted larval growth on a poor diet. A bacterial genome-wide association study (GWAS) demonstrated that 23 pathways in bacteria were positively associated with host larval growth (indicated by body length). Further analysis revealed that the vitamin B6 synthesis pathway in symbiotic bacteria was the key pathway regulating larval growth.

Results

Microbial diversity decreases during *B. dorsalis* larval development

We first investigated the gut microbiota diversity of 3-instar larvae of *B. dorsalis*, including first-third instars (Supplementary Figure S1) [39]. We performed 16S rRNA sequencing of the samples of these 3 different instars collected from the laboratory. The results revealed that the number of OTUs shared by all three

instars was 700 out of the total 2002 OTUs, indicating that approximately 35% of the OTUs were relatively stable in the larval guts of 3 different instars and that the guts of the first instars had a greater number of OTUs than did those of the other 2 instars (Fig. 1a). The results of the UniFrac nonmetric multidimensional scaling (NMDS) analysis also revealed differences in the intestinal microbial communities among the 3 different instars. Unweighted UniFrac NMDS analysis revealed

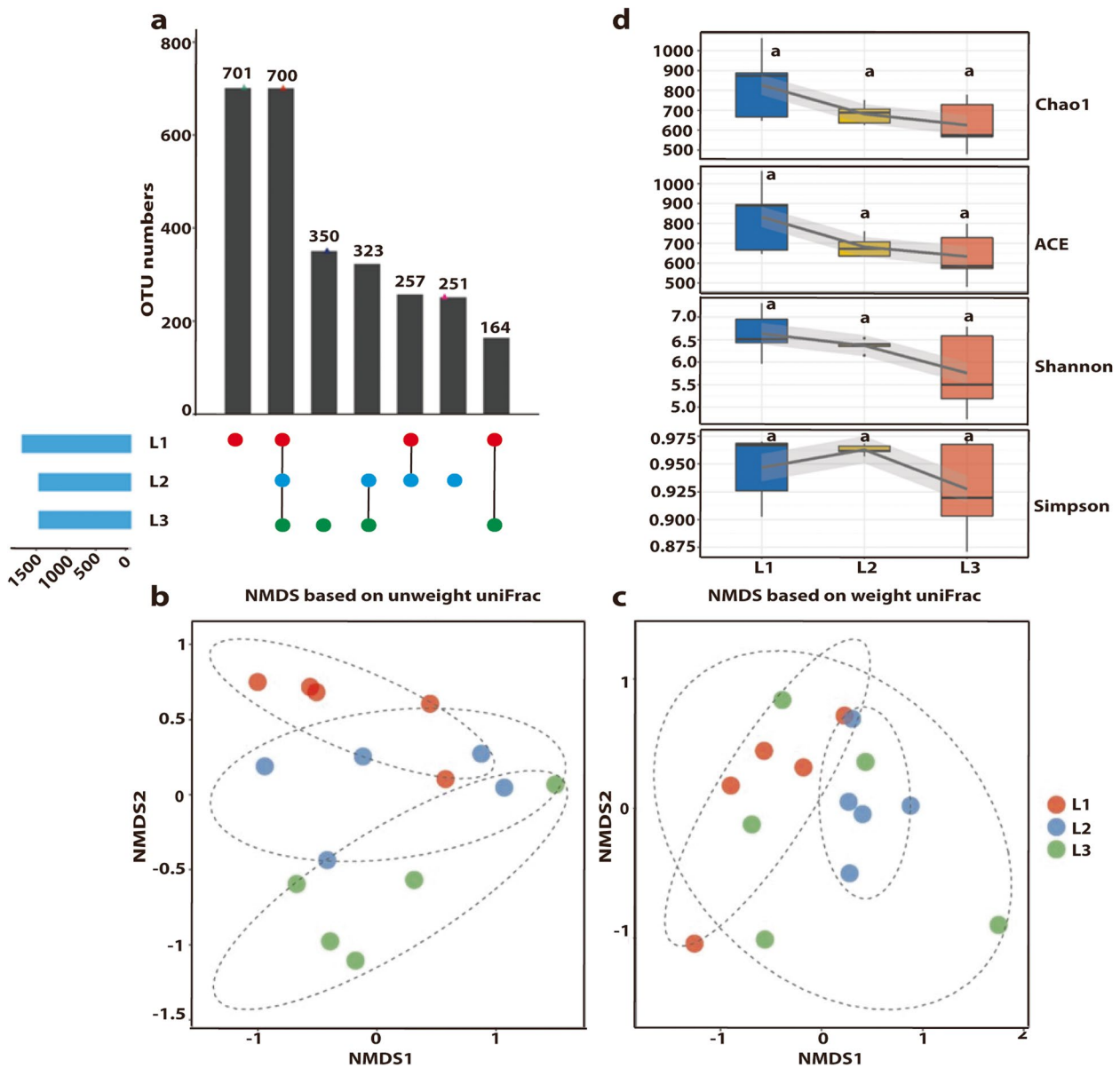


Fig. 1 Diversity analysis of the intestinal microbial community in larvae of 3 different instars. **a** Distribution of the common OTUs shared by 3 different instars and the unique OTUs specific to certain instars. **b** NMDS analysis based on unweighted UniFrac distance. **c** NMDS analysis based on weighted UniFrac distance. **d** Chao1 diversity index, ACE diversity index, Shannon diversity index, Simpson diversity index. L1, Instar 1 larva; L2, Instar 2 larva; L3, Instar 3 larva. Multiple comparisons were performed for each of the two groups. Letters indicate significant differences among groups ($p < 0.05$, one-way ANOVA, Tukey's post hoc test)

that the gut microbiota of the first- and third-instar larvae belonged to two different clusters (Fig. 1b). The weighted UniFrac NMDS analysis suggested that the first- and second-instar samples were separated, but the third instar samples were not clearly distinguished from the other two samples (Fig. 1c). Taken together, these results indicated that low-abundance microbial communities were instar specific. However, high-abundance species tended to be found in all three instars, suggesting a relatively high stability.

Next, we analyzed the alpha diversity of the gut microbial communities of larvae at three different instars. The results revealed that microbial diversity, as indicated by the Chao1, ACE, Shannon, and Simpson metrics, tended to decrease from L1 to L3, but there were no significant differences among the 3 instars (Fig. 1d).

Composition of the gut microbial community in *B. dorsalis* larvae

Furthermore, we examined the composition of the gut microbial community in the larvae of *B. dorsalis* and found that the larval gut microbiota was mainly composed of Proteobacteria, Firmicutes, Bacteroidetes, and Actinobacteria at the phylum level (Fig. 2a). We also analyzed the relative abundance of bacteria at the family level. The results revealed that Enterobacteriaceae and Streptococcaceae presented high relative abundances in the larval gut of all three instars (Instar 1, L1; Instar 2, L2; and Instar 3, L3), indicating their stability (Fig. 2b). Further analysis revealed that the relative abundance of Enterobacteriaceae was significantly greater in the second-instar larvae ($52.70\% \pm 2.541$) than in the first-instar larvae ($28.55\% \pm 3.716$) (Fig. 2c). The relative abundance of Leuconostocaceae in the gut also increased significantly during development, with its relative abundance in the third-instar larvae being significantly greater than that in the first-instar larvae (Fig. 2c).

In contrast, some microbiota families exhibited a clear decreasing trend with larval development. The relative abundances of the Streptococcaceae, Bacillaceae, Oxalobacteraceae, and Carnobacteriaceae families were significantly lower in the L3 than in the L1 larvae (Fig. 2d). The relative abundances of Brucellaceae, Acetobacteraceae, Pseudomonadaceae, Moraxellaceae, and Pseudonocardiaceae were not significantly different in the gut during larval development but still clearly decreased (Supplementary Figure S2d). In general, our results indicated that the abundances of Enterobacteriaceae and Leuconostocaceae did not strongly decrease during *B. dorsalis* larval development, suggesting their important role in larval growth and development of *B. dorsalis*.

Composition of cultivable bacterial communities in larvae of *B. dorsalis*

To further verify the above results, we cultured and isolated cultivable bacterial species using NA (a nonselective medium), VRBG (a selective medium for *Enterobacteriaceae*), and MRS (a selective medium for *Lactobacilli*) (Supplementary Figures S2a–c). We obtained 246 strains from NA medium (L1:96, L2:65, and L3:85) (Supplementary Table S1), 266 strains from VRBG medium (L1:72, L2:97, and L3:97) (Supplementary Table S2), and 158 strains from MRS medium (L1:71, L2:26, and L3:61) (Supplementary Table S3). To monitor changes in the intestinal bacterial composition at different instars, we monitored bacterial counts on a specific bacterial medium plate. In L1-NA, *Providencia rettgeri* and *Morganella morganii subsp. sibirica* accounted for 52.08% and 43.75% of the intestinal bacterial composition (Fig. 2e), respectively. In L2-NA, *M. morganii subsp. sibirica* was a relatively high-abundance species (58.46%) (Fig. 2f). Notably, the abundance of *Providencia alcalifaciens* increased from 1.04% (at L1) to 29.23% [at L2]). In L3-NA, *P. rettgeri* accounted for 32.94%, *E. cloacae* accounted for 24.71%, and *M. morganii subsp. sibirica* accounted for 24.71% of the intestinal bacterial composition (Fig. 2g). These findings were in accordance with the alpha diversity analysis results, which revealed that high-abundance species were relatively stable, whereas low-abundance species were less stable.

We observed similar results in the VRBG medium. In L1-VRBG, we identified *M. morganii subsp. sibirica* (55.56%) and *P. rettgeri* (44.44%) (Fig. 2h). In L2-VRBG, we observed *M. morganii subsp. sibirica* (77.73%) and *P. alcalifaciens* (22.68%) (Fig. 2i). In L3-VRBG, we detected *P. rettgeri* (43.30%), *M. morganii subsp. sibirica* (24.74%), and *P. alcalifaciens* (11.34%) (Fig. 2j). Collectively, these data indicated that Enterobacteriaceae were relatively stable during *B. dorsalis* larval development, supporting their important role in mediating larval growth.

Since *Lactobacillus* plays a crucial role in the growth of *Drosophila* and other animals [31–34], we cultured and isolated Lactobacillales using MRS selective medium, which is a selective medium for *Lactobacilli* and other species in the Lactobacillales. In L1-MRS, *Leuconostoc holzapfelii* accounted for 30.99%, *Fructobacillus duriensis* accounted for 28.17%, *Leuconostoc pseudomesenteroides* accounted for 11.27%, and *Fructobacillus fructosus* and *L. pseudomesenteroides* accounted for 25.35% and 11.27%, respectively, of the Lactobacillales (Fig. 2k). We also observed a change in the *Lactobacillus* bacterial composition in L2 larvae (Fig. 2l), with *F. fructosus* and *L. holzapfelii* making up the two dominant species accounting for more than 88% of the total culturable *Lactobacillus* bacteria. In L3-MRS medium (Fig. 2m),

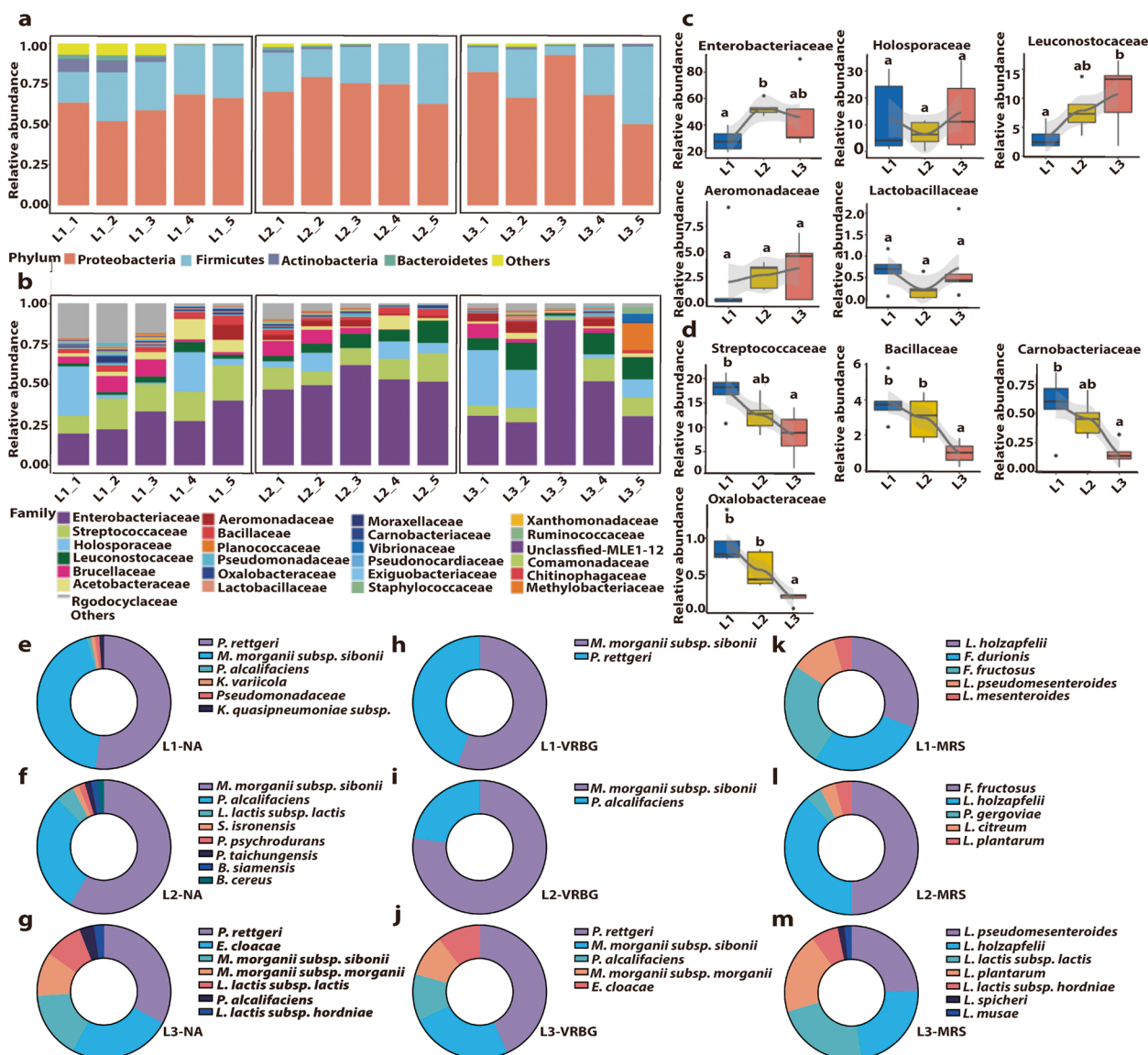


Fig. 2 Composition of the gut culturable microbiota in different instar larvae. **a** Gut microbiota composition at the phylum level in different instar larvae. **b** Gut microbiota composition at the family level in different instar larvae. L1-1, L1-2, L1-3, L1-4, and L1-5 represent the 5 biological replicates of instar-1 larvae; L2-1, L2-2, L2-3, L2-4, and L2-5 represent the 5 biological replicates of instar-2 larvae; and L3-1, L3-2, L3-3, L3-4, and L3-5 denote the 5 biological replicates of instar-3 larvae. **c** Relative abundance increases with increasing number of larval instars. **d** Relative abundance decreases with increasing number of larval instars. **e-g** Gut culturable microbiota composition of L1, L2, L3 on NA medium. **h-j** Gut culturable microbiota composition of L1, L2, L3 on VRBG medium. **k-m** Gut culturable microbiota composition of L1, L2, L3 on MRS medium. Multiple comparisons were performed for each of the two groups. Different letters indicate significant differences among groups at different instars ($p < 0.05$, one-way ANOVA, Tukey's post hoc test)

L. pseudomesenteroides accounted for 24.59% and *L. holzapfelii* accounted for 22.95% of the total culturable *Lactobacillus* bacteria. In general, *Providencia* and *Morganella*, which belong to the *Enterobacteriaceae*, and *Leuconostoc*, a member of the *Leuconostocaceae*, were the dominant cultivable bacteria that were stably present in the gut of *B. dorsalis* larvae. In summary, an investigation of the intestinal bacterial abundance of *B. dorsalis* larvae

revealed that *Enterobacteriaceae* and *Leuconostoc* might play important roles in the growth and development of *B. dorsalis* larvae.

Single bacterium replenishment promotes larval growth

We raised axenic larvae (AX group) and conventional larvae (CK group) on an artificial diet supplemented with 0.4% yeast. The results revealed that larvae in the AX

group presented significantly shorter body lengths and body weights than those in the CK group fed a diet with 0.4% yeast. Replenishment with culturable microbiota (AXA) partially rescued the axenic larval body lengths and body weights (Fig. 3b, c; Supplementary Figure S3).

Next, we performed monoassociation experiments to decipher the mechanism by which the microbiota promoted larval growth (Fig. 3a). We selected a total of 27 bacterial strains, including 21 *B. dorsalis* gut bacterial strains (isolated in this study and those from the laboratory stock) and 6 strains from the *B. dorsalis* habitat (previous laboratory stock) (Table 1). The larvae were raised on a 0.4% yeast diet, and their length was measured on Day 6. The results revealed that the average larval length in the AX group was 3.79 ± 0.10 mm and that in the AXA group was 6.71 ± 0.16 mm, which was significantly greater than that in the AX group. A monoassociation experiment revealed that 14 out of 27 tested strains

significantly promoted AX larval body length (Fig. 3b; Supplementary Figure S3), and 16 strains significantly promoted AX larval body weight (Fig. 3c). Among these 14 strains, AX larvae monoassociated with *E. cloacae* (N29), *M. morgani* (V41), *P. alcalifaciens* (V29), and *E. hormaechei* (EH) (larvae fed diets supplemented with one single strain) were significantly longer than AXA larvae supplemented with total gut bacteria, indicating that these strains had a greater impact on larval growth (Fig. 3b). *E. cloacae* (N29) had the most prominent effect, and the AX larvae monoassociated with this bacterium were more than twice the length of those in the AX group without strain replenishment and significantly promoted weight gain of larvae compared those in the AX group (Fig. 3c). Moreover, the symbiotic bacterium *Lactobacillus L. plantarum* (M96) significantly promoted the growth of larvae (Fig. 3b, c), and the nonsymbiotic bacterium *Escherichia coli* (EC) also significantly promoted

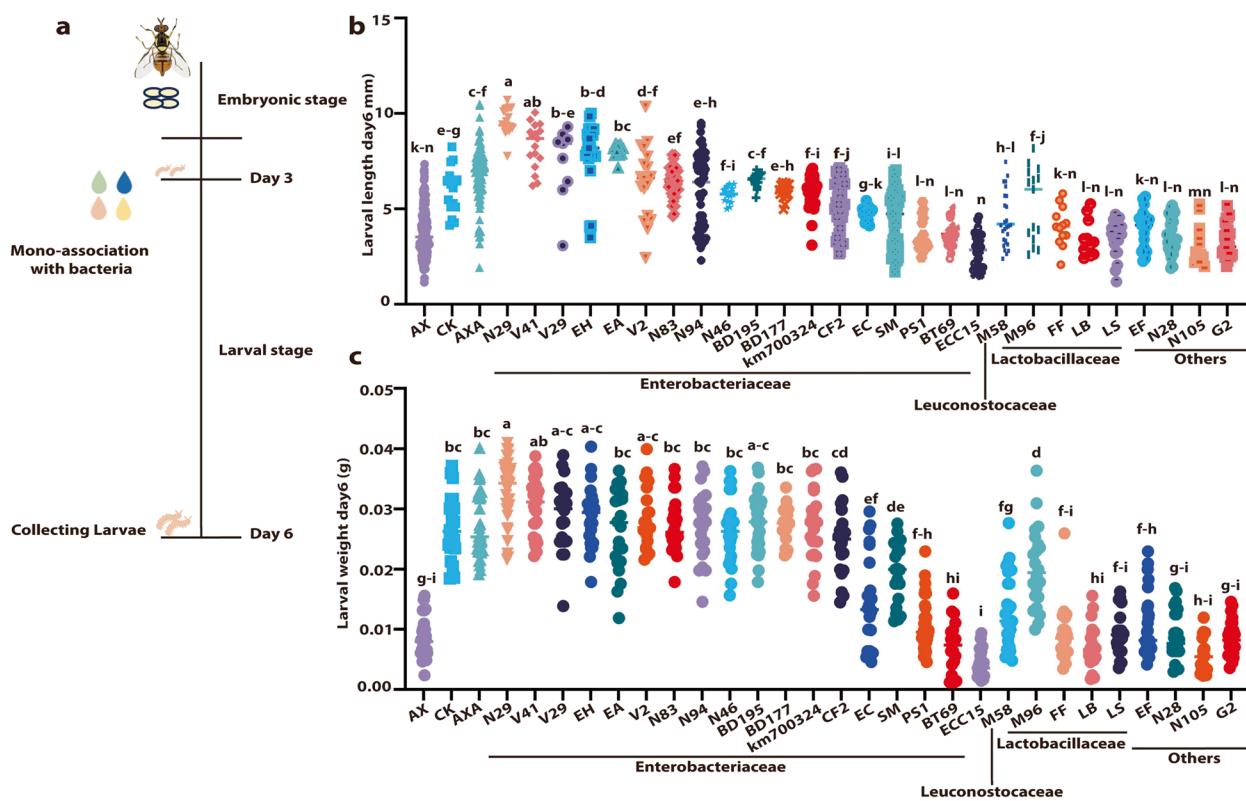


Fig. 3 Effects of 27 bacterial strains monoassociated with larvae on larval growth. **a** Schematic diagram of bacterial strains associated with larvae. **b** Larval longitudinal length after inoculation with AX ($n = 161$), CK ($n = 17$), AXA ($n = 95$), N29 ($n = 18$), V41 ($n = 17$), V29 ($n = 9$), EH ($n = 25$), EA ($n = 10$), V2 ($n = 18$), N83 ($n = 35$), N94 ($n = 65$), N46 ($n = 19$), BD195 ($n = 17$), BD177 ($n = 18$), km700324 ($n = 29$), CF2 ($n = 47$), EC ($n = 18$), M96 ($n = 15$), M58 ($n = 27$), SM ($n = 65$), PS1 ($n = 18$), EF ($n = 13$), LB ($n = 12$), LS ($n = 24$), N28 ($n = 40$), G2 ($n = 26$), BT69 ($n = 21$), ECC15 ($n = 27$), and N105 ($n = 14$). **c** Larval longitudinal weight after inoculation with AX ($n = 29$), CK ($n = 23$), AXA ($n = 35$), N29 ($n = 44$), V41 ($n = 28$), V29 ($n = 22$), EH ($n = 26$), EA ($n = 23$), V2 ($n = 21$), N83 ($n = 24$), N94 ($n = 21$), N46 ($n = 23$), BD195 ($n = 30$), BD177 ($n = 22$), km700324 ($n = 23$), CF2 ($n = 22$), EC ($n = 24$), M96 ($n = 22$), M58 ($n = 27$), SM ($n = 21$), PS1 ($n = 34$), EF ($n = 27$), LB ($n = 20$), LS ($n = 24$), N28 ($n = 24$), G2 ($n = 24$), BT69 ($n = 18$), ECC15 ($n = 21$), and N105 ($n = 22$). AXA, Axenic larvae on a diet supplemented with the total gut microbiota; AX, Axenic larvae; CK, control group (refers to flies with a 0.4% yeast diet). Multiple comparisons were performed for each of the two groups. Different letters indicate significant differences among groups at different instars ($p < 0.05$, one-way ANOVA, Tukey's post hoc test)

Table 1 Candidate bacterium strains of mono-associated axenic larvae

Strain	Resource	Classification level
BD177	<i>Bactrocera dorsalis</i>	<i>Klebsiella michiganensis</i>
BD195	<i>Bactrocera dorsalis</i>	<i>Citrobacter koseri</i>
BT68	<i>Zelugodacus tau</i>	<i>Providencia stuartii</i>
CF2	<i>Zelugodacus tau</i>	<i>Citrobacter portucalensis</i>
EA	<i>Bactrocera dorsalis</i>	<i>Enterobacter soli</i>
EC	DH5a strain	<i>Escherichia coli</i>
ECC15	<i>Drosophila melanogaster</i>	<i>Erwinia carotovora</i>
EF	<i>Bactrocera dorsalis</i>	<i>Enterococcus faecalis</i>
EH	<i>Bactrocera dorsalis</i>	<i>Enterobacter hormaechei</i>
FF	<i>Bactrocera dorsalis</i>	<i>Fructobacillus fructosus</i>
G2	<i>Bactrocera dorsalis</i>	<i>Agrobacterium fabrum</i>
km700324	ATCC	<i>Klebsiella michiganensis</i>
LB	<i>Bactrocera dorsalis</i>	<i>Lactobacillus brevis</i>
LS	<i>Bactrocera dorsalis</i>	<i>Lactobacillus spicheri</i>
M58	<i>Bactrocera dorsalis</i>	<i>Leuconostoc citreum</i>
M96	<i>Bactrocera dorsalis</i>	<i>Lactobacillus plantarum</i>
N105	<i>Bactrocera dorsalis</i>	<i>Psychrobacillus soli</i>
N28	<i>Bactrocera dorsalis</i>	<i>Paenibacillus pabuli</i>
N29	<i>Bactrocera dorsalis</i>	<i>Enterobacter cloacae</i>
N46	<i>Bactrocera dorsalis</i>	<i>Klebsiella quasipneumoniae</i>
N83	<i>Bactrocera dorsalis</i>	<i>Providencia stuartii</i>
N94	<i>Bactrocera dorsalis</i>	<i>Morganella morganii</i>
PS1	<i>Phyllotreta striolata</i>	<i>Serratia marcescens</i>
SM	<i>Bactrocera dorsalis</i>	<i>Serratia nematodiphila</i>
V2	<i>Bactrocera dorsalis</i>	<i>Providencia rettgeri</i>
V29	<i>Bactrocera dorsalis</i>	<i>Providencia alcalifaciens</i>
V41	<i>Bactrocera dorsalis</i>	<i>Morganella morganii</i>

the body weight of larvae (Fig. 3b). The pathogenic bacteria *Serratia marcescens* (PS1), *Providencia stuartii* (BT69), *Erwinia carotovora* Ecc15, and *Psychrobacillus soli* (N105) had no significant effect on larval growth. In general, all the *Enterobacteriaceae* strains and *Lactobacillus* strain *L. plantarum* (M96) isolated from the intestine of *B. dorsalis* promoted larval growth, whereas other symbiotic bacteria and pathogenic bacteria had no effect on larval growth.

Genome-wide association study of intestinal bacterial strains of *B. dorsalis*

To investigate the effects of bacteria on host larval growth, we performed genome sequencing of these 27 strains. The phylogenetic tree constructed using the maximum likelihood method revealed that *Klebsiella*, *Providencia*, *Morganella*, *Citrobacter*, *Serratia*, *Erwinia*, and *Escherichia* were closely related to each other and belonged to the *Enterobacteriaceae* (Fig. 4a). *Psychrobacter*, *Paenibacillus*, and *Agrobacterium* were clustered together, and they belonged to the *lactobacilli* (lactic acid-producing bacteria), but they were far from the *Enterobacteriaceae*. The above evolutionary relationships might explain the differences in the ability to promote larval growth in *B. dorsalis*.

Next, we analyzed the associations between bacterial genome sequences and larval growth-promoting ability under poor dietary conditions. Our bacterial genome-wide association study (GWAS) results revealed that 5512 orthologous genes were significantly associated with body length. Among these genes, 3417 were positively associated with larval body length. GO enrichment analysis revealed that these 3417 orthologous genes

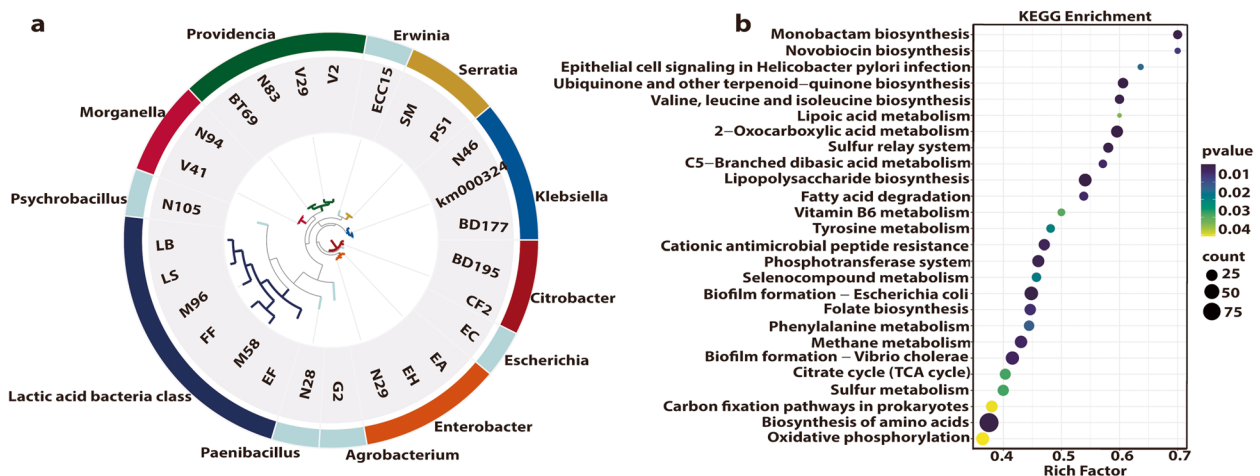


Fig. 4 Bioinformatics analysis of the intestinal bacterial genomes of *B. dorsalis* larvae. **a** Phylogenetic tree of 27 strains. A total of 1904 single-copy genes in the 27 strain genomes were concatenated, and the total length of the amino acid sequence was 15,742. **b** KEGG functional enrichment analysis of 3417 directly homologous genes that were significantly and positively associated with larval growth

were associated with GO terms such as ion transport and binding, amino acid metabolism, membrane structure composition, redox reactions, and the respiratory chain, and these GO terms were related mainly to amino acids, micronutrients, and energy metabolism, which are required for larval growth and development (Supplementary Figure S4).

KEGG pathway enrichment analysis revealed that all 3417 genes were enriched in 23 pathways, such as tyrosine metabolism, vitamin B6 synthesis, valine, leucine, isoleucine biosynthesis, and folate biosynthesis (Fig. 4b). The five KEGG pathways associated with the largest number of genes were the amino acid biosynthesis pathway, biofilm formation by *Vibrio cholerae*, biofilm formation by *Escherichia coli*, the lipopolysaccharide biosynthesis pathway, and the oxidative phosphorylation pathway (Fig. 4b). Notably, some pathways, such as biofilm formation and lipopolysaccharide biosynthesis, were highly enriched, suggesting that successful colonization or the formation of microbiota were important for host-microbe interactions.

***E. cloacae* N29 promotes larval growth by producing vitamin B6**

Our data showed that *E. cloacae* N29 had the most significant promoting effect on larval growth under limited yeast diet conditions. From the host perspective, the essential nutrients provided by the microbiota could be a more direct way to affect larval growth. Since yeast powders are rich in amino acids, vitamin B, and trace elements, we investigated 4 biosynthesis pathways, including valine, leucine and isoleucine, vitamin B6, and folate biosynthesis pathways, in *E. cloacae* N29. A total of 4 total responsible for the abovementioned 4 biosynthesis pathways were screened via the R package ClusterProfiler [40] in the *E. cloacae* N29 genome, and 8 *E. cloacae* N29 single mutants were generated by deleting each of these genes (Table 2). To further reveal the roles of each

of these four pathways in larval growth and development, we performed monoassociation experiments with these 8 mutant strains. The results revealed that axenic larvae fed diets supplemented with the $\Delta YcgM$, $\Delta trpE$, $\Delta pdxA2$, $\Delta IlvA$, $\Delta TdcB$, $\Delta pabB$, and $\Delta hpcE$ mutant strains successfully recovered body length and weight (Fig. 5a, b; Supplementary Figure S5a). However, supplementation with the $\Delta pdxA$ mutant strains in the axenic larval diet resulted in no significant difference in larval body length or weight, indicating that the *E. cloacae* N29 *pdxA* knockout strain lost the ability to promote larval growth (Fig. 5a, b; Supplementary Figure S5a). Since the *pdxA* gene belongs to the vitamin B6 biosynthesis pathway, our findings showed that vitamin B6 biosynthesis played an important role in promoting *B. dorsalis* larval growth.

Furthermore, we explored whether *E. cloacae* N29 could promote larval growth by producing vitamin B6 (Fig. 5c). Moreover, the growth of *E. cloacae* N29 and the $\Delta pdxA$ mutant were similar in the LB medium, indicating that the inability of the $\Delta pdxA$ mutant to increase larval size was not due to its own growth defect (Fig. 5d). We subsequently attempted to rescue the phenotype of larval body length and weight by co-feeding *B. dorsalis* axenic larvae with the *E. cloacae* N29 $\Delta pdxA$ mutant and vitamin B6. The results showed that the addition of vitamin B6 successfully restored the ability of the *E. cloacae* N29 $\Delta pdxA$ mutant to rescue larval body length and weight, indicating that *E. cloacae* N29 promoted larval growth by increasing vitamin B6 synthesis via *pdxA* (Fig. 5e, f; Supplementary Figure S5b).

Discussion

Here, we found that intestinal commensal bacteria promoted *B. dorsalis* larval growth under poor nutritional conditions and that this promotion effect was not limited to a single bacterial species. Our GWAS revealed that microbiota genes positively associated with host larval growth were enriched in several physiological pathways.

Table 2 Candidate KEGG pathways and probiotic genes in N29 strain

KEGG ID	Description	P value	Orthogroup ID	N29_gene ID	annotation
map00290	Valine, leucine and isoleucine biosynthesis	0.000761	OG0000271	N29_01495	L-threonine dehydratase catabolic <i>TdcB</i>
				N29_04636	L-threonine dehydratase biosynthetic <i>IlvA</i>
map00350	Tyrosine metabolism	0.019887	OG0000095	N29_00056	putative protein <i>YcgM</i>
				N29_03535	Homoprotocatechuate catabolism bifunctional isomerase/decarboxylase <i>hpcE</i>
map00750	Vitamin B6 biosynthesis	0.029715	OG0000499	N29_01801	D-threonate 4-phosphate dehydrogenase <i>pdxA2</i>
				N29_03442	4-hydroxythreonine-4-phosphate dehydrogenase <i>pdxA</i>
map00790	Folate biosynthesis	0.0052	OG0000186	N29_00068	Aminodeoxychorismate synthase component 1 <i>pabB</i>
				N29_02137	Anthranilate synthase component 1 <i>trpE</i>

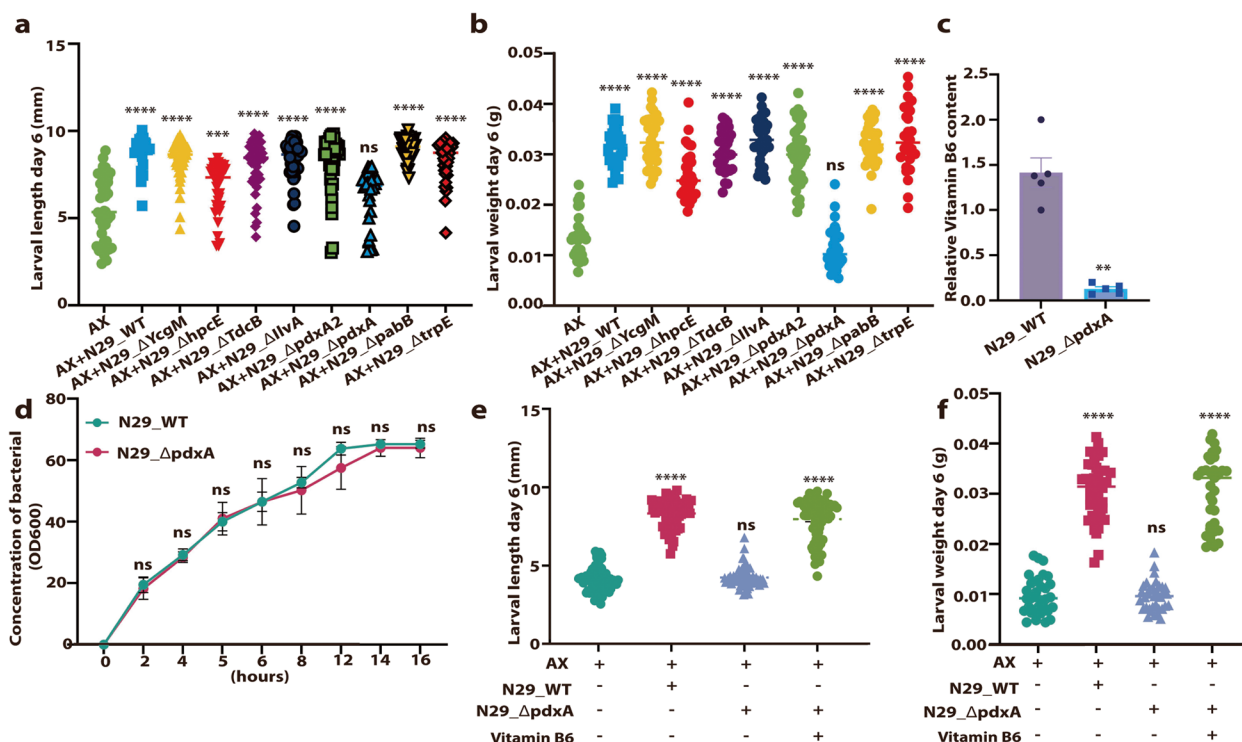


Fig. 5 Effects of the deletion of 8 genes in the N29 mutant strain on larval growth. **a** Body length of 6-day-old larvae mono-associated with different N29 mutant strains. Larval longitudinal length after inoculation with AX ($n = 41$), N29_WT ($n = 21$), N29_ΔTdcB ($n = 42$), N29_ΔIlvA ($n = 43$), N29_ΔYcgM ($n = 54$), N29_ΔhpcE ($n = 44$), N29_ΔpdxA2 ($n = 39$), N29_ΔpdxA ($n = 27$), N29_ΔpabB ($n = 47$), and N29_ΔtrpE ($n = 42$). **b** Larval weight after inoculation with AX ($n = 30$), N29_WT ($n = 28$), N29_ΔTdcB ($n = 33$), N29_ΔIlvA ($n = 39$), N29_ΔYcgM ($n = 34$), N29_ΔhpcE ($n = 35$), N29_ΔpdxA2 ($n = 41$), N29_ΔpdxA ($n = 32$), N29_ΔpabB ($n = 32$), and N29_ΔtrpE ($n = 26$); each data point represents the total weight of the three larvae. **c** Relative vitamin B6 content of N29_WT and N29_ΔpdxA. The values are normalized ratios of the relative vitamin B6 content (with one sample in N29_WT set as one, and all other values are displayed as normalized ratios). **d** Growth curves of the N29_WT and N29_ΔpdxA strains. **e** Body length of 6-day-old larvae in 4 groups: AX larvae ($n = 33$), AX+N29_WT ($n = 42$), AX+N29_ΔpdxA ($n = 35$), and AX+N29_ΔpdxA+vitamin B6 ($n = 33$). **f** Larval weight after inoculation with AX larvae ($n = 65$), AX+N29_WT ($n = 62$), AX+N29_ΔpdxA ($n = 65$) and AX+N29_ΔpdxA+Vitamin B6 ($n = 77$). Each data point represents the total weight of three larvae. The differences in mean body length of the larvae were compared between the treatment groups and the AX group using the Student's *t* test. *, $P < 0.05$; **, $P < 0.001$; ****, $P < 0.0001$; ns, not statistically significant

We further demonstrated that *E. cloacae* N29 promoted host larval growth by regulating *pdxA*-mediated vitamin B6 biosynthesis. In summary, our data revealed the important role of the gut microbiota in the larval growth of *B. dorsalis*.

We found that *B. dorsalis* larvae harbored many stage-specific low-abundance microbial communities. In contrast, high-abundance microbial communities were relatively stable in different larval stages. Our data revealed that Enterobacteriaceae and Leuconostocaceae were the most dominant species present in the *B. dorsalis* larval gut. Similarly, a previous study also found that Enterobacteriaceae was the dominant bacterial species in the *B. dorsalis* larval gut in different geographic populations and under different rearing conditions [41]. Vertical transmission of insect microorganisms is a well-adapted strategy for the environment. Like *B. dorsalis* larvae, Enterobacteriaceae are also the main dominant species in

adult *B. dorsalis*, including some *Citrobacter*, *Klebsiella*, *Providencia*, and *Enterobacter* species [36, 42–44], and they are known to be transmitted vertically by parental deposition of the bacteria on the egg surface. Therefore, although *B. dorsalis* larvae presented a decreased microbiota diversity, this feature may be rescued by adult development, allowing the successful passage of the microbiota to the progeny. In *B. minax*, the increase in abundance of Leuconostocaceae during development has been reported to be associated with fructose and mannose metabolic activities in the intestinal tract [45]. In many insects, Enterobacteriaceae is a common bacterial species that affects host metabolism, immunity, and reproduction [46–51].

Therefore, we speculated that this gene might play an important role in *B. dorsalis* larval development.

We found that multiple microbial species rather than a single species were required for larval growth on a

poor diet. Indeed, many studies have shown that the microbiota can facilitate insect growth under nutrient-deficient conditions. Germ-free *Drosophila* larvae grow more slowly and are smaller in size when fed a poor diet. Monoassociation with either one of two commensal bacteria, *Acetobacter pomorum* or *Lactobacillus plantarum*, promotes larval growth through the TOR and insulin pathways [32, 33, 52]. It has been widely reported that the microbiota produces numerous growth-promoting factors in *Drosophila* models [31, 34, 53, 54]. Similar phenotypes have also been observed in other insects, such as *A. mellifera* [55] and *Ceratitidis capitata* [56]. In the beetle *Holotrichia parallela*, the microbiota participates in host metabolism and provides nutrients for the host by degrading cellulose and hemicellulose [57–60]. Our previous study reported that gut fungi also have a probiotic function in *B. dorsalis* [61]. However, existing studies have focused on only a few microbiota species and their functions in larval development. In this study, we found that at least a dozen microbiota species promoted larval development in *B. dorsalis*. Our GWAS results also suggested that multiple bacterial physiological pathways might be responsible for host development under nutrient deficiency conditions. For example, two biofilm formation pathways among the top five enriched pathways were positively associated with larval growth, suggesting that biofilm formation by the microbiota could be the key factor regulating this host-microbe relationship in *B. dorsalis*. Several studies have confirmed the necessity for biofilm formation in gut microbiota colonization [62–66]. Interestingly, a recent study reported that outer membrane vesicle (OMV) biogenesis and biofilm-like aggregates enhance mosquito commensal bacterium colonization and the resistance of the host to *Plasmodium* [67].

B vitamins are growth-promoting factors that are critical to the main metabolism of animals [53]. However, vitamin B cannot be synthesized by animals; it is obtained from the environment or synthesized by the microbiota [68]. The microbiota of *Drosophila* can provide larvae with riboflavin, thiamine, and pantothenate to promote growth [28, 34, 54, 69]. In addition, riboflavin biosynthesis is an important function of the gut microbiota in *A. aegypti* larvae [70]. Vitamin B provided by the microbiota is involved in promoting *Glossina* development and reproduction [71]. Our study revealed that vitamin B6 biosynthesis by the microbiota was essential for promoting larval growth in *B. dorsalis*. The *pdxA* gene is mainly responsible for the biosynthesis of vitamin B6. The *pdxA*-deleted *E. cloacae* N29 mutant could not biosynthesize vitamin B6; thus, this mutant lost its ability to promote host larval growth. Vitamin B6 exists in six main forms, and pyridoxal-5'-phosphate, as one

of the main active forms of vitamin B6, is an important cofactor for more than 140 enzymes [71]. Similar to our observations, many bacteria, such as *A. pomorum*, *L. plantarum*, *E. coli*, and *Rhodococcus rhodnii*, are predicted to have a complete vitamin B6 biosynthesis pathway in their genomes [71]. In tsetse flies, vitamin B6 produced by the symbiotic bacteria *Wigglesworthia glossinidia* is important for maintaining host proline homeostasis and fecundity [72]. In other insects, such as aphids, bedbugs, kissing bugs, and ticks, dietary supplementation with vitamin B6 partially rescues the phenotype defects associated with larval development [71]. In this study, we found that of the 14 strains that promoted larval growth, *E. cloacae* N29 exhibited the most prominent promoting effect on larval growth in *B. dorsalis*. We speculated that the growth-promoting effects of the 13 others bacterial species could also rely on vitamin B6 synthesis, suggesting a potentially redundant role of the microbiota in supporting larval growth.

In summary, our data demonstrate that multiple microbiota species can promote larval development in the fruit fly *B. dorsalis* and reveal the key role of vitamin B6 biosynthesis in promoting *B. dorsalis* larval growth. KEGG analysis revealed that multiple pathways, especially the amino acid, lipopolysaccharide, fatty acid, and oxidative phosphorylation pathways, potentially promoted larval growth in *B. dorsalis*. Our work provides a foundation for further functional studies focusing on insect-microbe relationships in more complex scenarios with multiple bacteria species-host interactions.

Materials and methods

Insect rearing

The experimental insects were collected from Guangdong Province, China, using protein bait, and they were maintained at the Institute of Urban and Horticultural Insects, Huazhong Agricultural University, Wuhan, Hubei, China. The photoperiod of the insect-rearing room was 12-h light:12-h dark. The room's relative humidity was 70–80%, and the temperature was maintained at 28 ± 1 °C. Larvae were fed larval food (wheat bran, 80 g; corn flour, 40 g; sucrose, 40 g; yeast powder, 15 g; water, 200 ml). After eclosion, the adult flies were moved to 30 cm × 30 cm × 30 cm cages. Adult flies were raised on a mixture of sucrose and yeast at a ratio of 3:1.

Preparation of larval gut samples

The larvae were subsequently rinsed in 75% alcohol for 3 min, followed by three rinses in sterile water. An appropriate amount of sterile PBS buffer was added to a sterile Petri dish. The larvae were dissected with sterile forceps under a stereomicroscope to obtain gut samples. The resulting gut samples were used for total DNA extraction

and the detection and isolation of culturable bacteria. There were 5 biological replicates for each instar larval gut sample, with 30 larval gut tissues per biological replicate.

Bacterial DNA extraction and 16S rDNA amplicon sequencing

Bacterial DNA was extracted from each instar larval gut sample using an E.Z.N.A.[®] Soil DNA Kit (Omega, Norcross, GA, USA) according to the manufacturer's instructions, with five biological replicates. The variable region V3 + V4 of the 16S rRNA gene was amplified via a broad-range primer pair (338F: 5'—ACTCCTACGGGAGGCA—3', 806R:5'—GGACTACHVGGGTWTCTAAT—3') using Phusion[®] High-Fidelity PCR Master Mix (New England Biolabs, Beverly, MA, USA). The PCR amplification program was as follows: preincubation at 95 °C for 5 min; 35 cycles at 56 °C for 45 s, at 72 °C for 1 min, and at 94 °C for 45 s; and a final extension at 72 °C for 10 min. The PCR products were subjected to PE300 double-end sequencing on the Illumina MiSeq sequencing platform.

Analysis of 16S rRNA gene amplicon data

To integrate the raw double-end sequencing data, FASTQ double-end sequences were filtered using the sliding window method, and the parameters were set as follows: the window size was 10 bp; the step size was 1 bp; the average quality score of the sequence in the window was $\geq Q20$; and the average sequencing accuracy of the base was $\geq 99\%$. Sequences with an average quality score lower than $Q20$ were truncated from the first window, and the truncated sequence length was ≥ 150 bp. The ambiguous base *N* was not allowed. After preliminary quality control, the paired-end sequences were connected pairwise on the basis of overlapping bases using FLASH software following the requirements that the overlapping base length between read 1 and read 2 was ≥ 10 bp and that base mismatches were not allowed. Finally, valid sequences for each sample were obtained. Chimeric sequences were removed using USEARCH. The resulting qualified sequences were merged and divided into different (operational taxonomic units) OTUs based on 97% sequence similarity using QIIME software. The sequence with the highest abundance in each OTU was selected as the representative sequence of that OTU. Based on the number of sequences contained in each OTU in each sample, a matrix file of the OTU abundance in each sample was subsequently constructed. By aligning the OTU representative sequence with the sequence in the Greengenes database, the taxonomic information was obtained for the corresponding OTU. Diversity indices, such as the Simpson index, Chao1 index, ACE index, and Shannon index, were calculated for each sample using

QIIME software. The relative abundance matrix at the genus level was submitted to the Galaxy online analysis platform for LEfSe analysis.

Isolation and identification of culturable bacteria from the larval gut

Each instar larval gut tissue sample was placed into a 1.5-ml centrifuge tube, and 1 ml of sterile PBS and an appropriate amount of sterile glass sand were added. The 10 larval gut tissue samples of each instar were homogenized, and then 100 μ l of the homogenate was subjected to gradient dilution (by 10×10^{-3} , 10^{-4} , 10^{-5} , and 10^{-6}). One hundred microlitres of the homogenate was coated onto nutrient agar (NA) medium and violet red bile glucose agar (VRBG) medium and cultured at 30 °C for 24–48 h under aerobic conditions or incubated on DeMan-Rogosa-Sharpe (MRS) medium at 30 °C for 24–48 h in an MGC-7L-sealed anaerobic incubator. Next, 100 single colonies were randomly selected from each of the three medium plates of gut tissue homogenate culture at 3 different instars (first–third) and placed in the corresponding liquid media (NA, VRBG, and MRS). The colonies were incubated in NA and VRBG liquid media at 200 r/min for 24 h at 30 °C, whereas the colonies incubated in MRS liquid media were incubated anaerobically for 24 h at 30 °C. After incubation, an equal volume of 40% glycerol was added to the resulting bacterial mixture, which was stored at -80 °C. Bacterial genomic DNA was extracted from the bacterial mixture using a HiPure Bacterial DNA Kit (Magen, Guangzhou, China).

Monoassociation experiment between bacteria and larvae

Preparation of related strains. Single colonies of isolated and identified strains were placed into the corresponding liquid media (NA, VRBG, and MRS) and cultured under appropriate conditions.

Quantification of bacteria in the bacterial mixture. After the bacterial mixture was diluted with a liquid medium at ratios of 1:1, 1:2, and 1:4, the OD600 value was measured. These diluted bacterial mixtures were coated onto solid media and cultured for 24 h, after which the number of colony-forming units (CFUs) was counted. The sterile water volume used to prepare the bacterial resuspension solution was calculated according to the following formula: $E = ((O - B) \times V \times D) / C$, where E is the volume of sterile water required for preparing the bacterial resuspension solution; O is the OD600 value of the cultured bacterial solution; B is the OD600 value of the blank culture solution; D is the dilution factor; and V is the volume of the bacterial suspension collected by centrifugation, and the above volume unit was expressed in microlitres (μ l).

Incubation of bacteria and larvae. One hundred microliters of the bacterial mixture were added to a sterile tube containing irradiation-sterilized larval feed and sterilized eggs and incubated in a constant-temperature incubator at 27 °C and 70% humidity for 6 days.

Determination of larval growth and development. Specifically, the feeding tube was opened, and the feed and larvae were poured into a Petri dish.

Larval body length measurements. The larvae were collected into EP tubes containing 50% glycerol with forceps. The larvae were subsequently placed on ice for 30 min and then laid freely on a black Petri dish and photographed with an Olympus stereoscope. The curved tool in ImageJ was used to draw the line in the middle of the larval body and measure its length.

Larval body weight measurements. The larvae were collected into centrifuge tubes and anesthetized by rapid freezing, with one replicate for every three total larval weights. Weighing was performed with an analytical balance.

Next-generation library construction and sequencing

Quality control of the bacterial genomic DNA was performed as follows. Agarose gel electrophoresis was used to analyze the purity and integrity of the DNA, and a NanoDrop 2000 Spectrophotometer (Thermo Fisher Scientific, Inc.) was used to detect the purity of the DNA (OD 260/280 ratio). Qubit 2.0 was used to determine the DNA concentration. After quality control, the bacterial genomic DNA samples were randomly disrupted with a Covaris ultrasonic breaker. Afterwards, a 350-bp library was constructed according to the following steps: end repair, addition of the A-tail, addition of a sequencing adapter, purification, and PCR amplification. The library concentration was subsequently measured using a Qubit 2.0 instrument and diluted, and the fragments inserted into the library were detected with an Agilent 2100 instrument. After the size of the inserted fragment met the requirements, the effective concentration of the library was quantified using the q-PCR method to ensure the library quality. Subsequently, the qualified library was subjected to PE150 sequencing on the Illumina NovaSeq 6000 high-throughput sequencing platform.

De novo genome assembly and annotation

The main steps for de novo genome assembly and annotation were as follows.

Illumina paired-end data were corrected and assembled via SPAdes software, and the numbers of contigs and dead ends were minimized after assembly. The contigs were further constructed into a genome scaffold diagram. According to the depth of the reads and the connectivity between the assembly diagrams, single-copy contigs were

distinguished from multicopy contigs using the greedy algorithm in the Unicycler software. The final genome assembly results for each strain were evaluated using QUAST software in terms of the number and length of contigs, the maximum contig number, and the N50 value in the assembled genome. The coding sequences, ribosomal RNA genes, transfer RNA genes, signal peptide genes, and noncoding RNA genes in the genome were annotated using Prokka software.

Whole-genome phylogenetic analysis

The fasta files of 27 strain genomes were converted into Anvi'o files, which were further converted into a single Anvi'o contig database. A single-copy gene HMM file was subsequently constructed, and the single-copy gene amino acid sequences of the 27 genomes were extracted from the HMM file. These sequences were concatenated and aligned to generate a fasta file. The amino acid sequences of the aligned single-copy genes were used to construct a phylogenetic tree.

Whole-genome association analysis of bacteria

The genomes of the larval intestinal strains were subjected to second-generation high-throughput sequencing, assembly, and annotation to obtain orthologous genes from the genomes of 27 strains. The statistical analyses of orthologous genes present in or absent from different strains and the larval body length data were performed using MAGNAMWAR in the R package. The orthologous genes significantly associated with the phenotype were screened by calculating the associations between the phenotype and the orthologous genes, with $p < 0.05$ as the screening threshold, to obtain an orthologous gene set. The orthologous gene sequences in all the larval intestinal strain genomes were functionally annotated using eggNOG-mapper software based on the eggNOG 5.0 database to obtain the GO and KEGG annotation information for the orthologous genes. GO and KEGG enrichment analyses of orthologous gene set that were significantly related to larval body length were performed using ClusterProfiler in the R package, with $p < 0.05$ as the enrichment analysis screening threshold.

Construction of bacterial mutant strains

We used the λ -Red homologous recombination system to knock out candidate bacterial genes. The specific procedures were as follows.

Preparation of N29 electroporation competent cells. The N29 strain was cultivated at 37 °C at 200 rpm/min until the OD600 reached 0.4–0.6. The bacterial mixture was centrifuged at a low temperature for 15 min. The strains were collected, resuspended in 30 ml of pre-cooled 10% glycerol, and stored in a –80 °C freezer. Fifty

nanograms of the pKD46 plasmid were added to 100 μ l of N29 electroporation-competent cells and mixed gently, and the mixture was transferred to a precooled electroshock cup. The electroshock cup was placed in the Bio-Rad electroporator for electroporation, with the voltage set to 1.8 kV. Then, 1 ml of LB was added to the culture, followed by shaking and recovery. The bacterial mixture was coated onto LB solid medium containing ampicillin and cultured at 30 °C overnight. Single colonies were collected from solid LB medium supplemented with ampicillin and cultured in LB liquid medium with shaking at 30 °C overnight. Lambda red induction reagent was added at a ratio of 1:200. The bacterial mixture was cultured with shaking until the OD600 reached approximately 0.4–0.6. The bacterial mixture was subsequently placed on ice for 30 min and centrifuged at low temperature for 15 min. The strains were collected, resuspended in 30 ml of precooled 10% glycerol, and stored in a –80 °C freezer. A 70-bp homologous recombination primer pair was designed. Of the 70 bp, 50 bp of the upstream and downstream primer pair consisted of a homologous sequence complementary to the gene to be knocked out, and the remaining 20 bp was complementary to the sequence of pKD4. Then, 500 ng of PCR product was added to 100 μ l of electroporation-competent cells and mixed gently, and the mixture was transferred to a precooled electroshock cup. The electroshock cup was placed in the Bio-Rad electroporator for electroporation, with the voltage set to 1.8 kV. One milliliter of LB was added to the culture for shaking and recovery, and then the bacterial mixture was coated onto LB solid medium containing kanamycin and cultured at 37 °C overnight. The genome of the mutant strain was extracted and PCR amplified using 20-bp primers (Supplementary Table S4).

Vitamin B6 content determination

One milliliter of bacterial culture medium was added to a 1.5-ml EP tube and centrifuged at 13,000 $\times g$ for 10 min. The 40 μ l of supernatant was collected for vitamin B6 content determination using a vitamin B6 content kit (Boxbio, Beijing, China) according to the manufacturer's instructions.

Fed vitamin B6 assay

A total of 200 μ l of 5 mg/ml vitamin B6 solution (Sangon Biotech, Shanghai, China) and the *pxxA*-deleted N29 mutant strain were co-fed to the larvae.

Data statistics and analysis

GraphPad Prism 9.0 software and R (3.6.3) were used for statistical analysis and visualization of the data. The differences between two independent samples were analyzed via a parametric Student's *t* test. Multiple

comparisons of multiple samples were performed using Tukey's multiple comparison method with one-way ANOVA, and $P < 0.05$ was considered statistically significant.

Supplementary Information

The online version contains supplementary material available at <https://doi.org/10.1186/s40168-024-01931-9>.

Supplementary Material 1: Supplementary Figure S1. Growth of larvae fed a banana diet. The body length of larva from day 3 to day 10 after egg laying. The data points represent the length of at least 20 larvae (mean \pm SE). L1: first-instar larva; L2: second-instar larva; L3: third-instar larva. Supplementary Figure S2. Changes in the microbiota in the gut of *B. dorsalis* larvae. (a) Colony morphology on NA medium. (b) Colony morphology on VRBG medium. (c) Colony morphology on MRS medium. (d) Relative abundance tended to decrease with increasing number of larval instars. Different letters indicate significant differences among groups at different instars ($p < 0.05$, one-way ANOVA, Tukey's post hoc test). Supplementary Figure S3. Size of sterile larvae 6 days after inoculation with 27 strains. AXA, Axenic larvae on a diet supplemented with the total gut microbiota; AX, Axenic larvae; CK, control group (CK refers to flies with a 0.4% yeast diet). The red line is the scale (3 mm). Supplementary Figure S4. Enrichment bubble plots for GO function. (a) Bubble map of cellular component level enrichment. (b) Bubble map of 8 simplified cellular components. (c) Bubble map of 16 biological processes identified via GO functional enrichment analysis. (d) Bubble map of simplified biological processes in the GO functional enrichment analysis. (e) Bubble map of 16 molecular function-related genes identified via GO functional enrichment analysis. (f) Bubble map of simplified molecular function levels from the GO functional enrichment analysis. Supplementary Figure S5. Size of sterile larvae 6 days after inoculation with N29 mutant strains. (a) Body size of 6-day-old larvae associated with different N29 mutant strains. (b) Body size of 6-day-old larvae fed N29_WT Δ PdxA or vitamin B6. The red line is the scale (3 mm). Supplementary Table S1. Proportion of intestinal microbiota of different instars in NA media. Supplementary Table S2. Proportion of intestinal microbiota of different instars in VRBG media. Supplementary Table S3. Proportion of intestinal microbiota of different instars in VRBG media. Supplementary Table S4. The primers used in the λ -red homologous recombination.

Acknowledgements

We extend our gratitude to all members of the Li and Zhang labs for their valuable suggestions on the project and their insightful discussions.

Authors' contribution

J.G., Z.C., H.Z. and X.L. designed whole study. J.G. wrote the main manuscript text. Z.Y. and B.L. made important suggestions and revised the manuscript. J.G. and Z.C. were collected sample. All authors reviewed the manuscript.

Funding

This study was supported by the National Natural Science Foundation of China (No. U21A20222, No. 32220103009), National Key R&D Program of China (No. 2021YFC2600400), China Agriculture Research System of MOF and MARA (CARS-26) and Hubei Hongshan Laboratory.

Data availability

Availability of supporting data Sequence files and metadata for all samples used in this study and all data supporting the main conclusions have been deposited in Figshare (DOI: <https://doi.org/10.6084/m9.figshare.25039781>).

Declarations

Ethics approval and consent to participate

Not applicable.

Consent for publication

Not applicable.

Competing interests

The authors declare no competing interests.

Received: 12 December 2023 Accepted: 13 September 2024

Published online: 04 November 2024

References

- Douglas AE. Multiorganismal insects: diversity and function of resident microorganisms. *Annu Rev Entomol.* 2015;60:17–34.
- Douglas AE. The molecular basis of bacterial–insect symbiosis. *J Mol Biol.* 2014;426:3830–7.
- Lemaitre B, Hoffmann J. The host defense of *Drosophila melanogaster*. *Annu Rev Immunol.* 2007;25:697–743.
- Gurung K, Wertheim B, Falcao SJ. The microbiome of pest insects: it is not just bacteria. *Entomol Exp Appl.* 2019;167:156–70.
- Cassone BJ, Grove HC, Elebute O, Villanueva SMP, LeMoine CMR. Role of the intestinal microbiome in low-density polyethylene degradation by caterpillar larvae of the greater wax moth, *Galleria mellonella*. *Proc Royal Soc B: Biol Sci.* 2020;287:20200112.
- Dunbar HE, Wilson ACC, Ferguson NR, Moran NA. Aphid thermal tolerance is governed by a point mutation in bacterial symbionts. *PLoS Biol.* 2007;5:e96.
- Oliver KM, Russell JA, Moran NA, Hunter MS. Facultative bacterial symbionts in aphids confer resistance to parasitic wasps. *Proc Natl Acad Sci USA.* 2003;100:1803–7.
- Oliver KM, Moran NA, Hunter MS. Variation in resistance to parasitism in aphids is due to symbionts not host genotype. *Proc Natl Acad Sci USA.* 2005;102:12795–800.
- Oliver KM, Degnan PH, Hunter MS, Moran NA. Bacteriophages encode factors required for protection in a symbiotic mutualism. *Science.* 2009;325:992–4.
- Oliver KM, Degnan PH, Burke GR, Moran NA. Facultative symbionts in aphids and the horizontal transfer of ecologically important traits. *Annu Rev Entomol.* 2010;55:247–66.
- Oliver KM, Smith AH, Russell JA. Defensive symbiosis in the real world – advancing ecological studies of heritable, protective bacteria in aphids and beyond. *Funct Ecol.* 2013;28:341.
- Scarborough CL, Ferrari J, Godfray HCJ. Aphid protected from pathogen by endosymbiont. *Science, New Series.* 2005;310:1781.
- Jamin AR, Vorburger C. Estimating costs of aphid resistance to parasitoids conferred by a protective strain of the bacterial endosymbiont *Regiella insecticola*. *Entomol Exp Appl.* 2019;167:252–60.
- Kikuchi Y, Hayatsu M, Hosokawa T, Nagayama A, Tago K, Fukatsu T. Symbiont-mediated insecticide resistance. *Proc Natl Acad Sci.* 2012;109:8618–22.
- Engl T, Eberl N, Gorse C, Krüger T, Schmidt THP, Plarre R, et al. Ancient symbiosis confers desiccation resistance to stored grain pest beetles. *Mol Ecol.* 2018;27:2095–108.
- Rothman JA, Leger L, Graystock P, Russell K, McFrederick QS. The bumble bee microbiome increases survival of bees exposed to selenate toxicity. *Environ Microbiol.* 2019;21:3417–29.
- Senderovich Y, Halpern M. The protective role of endogenous bacterial communities in chironomid egg masses and larvae. *ISME J.* 2013;7:2147–58.
- Douglas AE. Phloem-sap feeding by animals: problems and solutions. *J Exp Bot.* 2006;57:747–54.
- Sandström J, Pettersson J. Amino acid composition of phloem sap and the relation to intraspecific variation in pea aphid (*Acyrtosiphon pisum*) performance. *J Insect Physiol.* 1994;40:947–55.
- Baumann P. Biology of bacteriocyte-associated endosymbionts of plant sap-sucking insects. *Annu Rev Microbiol.* 2005;59:155–89.
- Douglas AE. Lessons from studying insect symbioses. *Cell Host Microbe.* 2011;10:359–67.
- Feng H, Edwards N, Anderson CMH, Althaus M, Duncan RP, Hsu Y-C, et al. Trading amino acids at the aphid–*Buchnera* symbiotic interface. *Proc Natl Acad Sci.* 2019;116:16003–11.
- Birkle LM, Minto LB, Douglas AE. Relating genotype and phenotype for tryptophan synthesis in an aphid–bacterial symbiosis. *Physiol Entomol.* 2002;27:302–6.
- Wu D, Daugherty SC, Van Aken SE, Pai GH, Watkins KL, Khouri H, et al. Metabolic complementarity and genomics of the dual bacterial symbiosis of sharpshooters. *PLoS Biol.* 2006;4:e188.
- Bennett GM, Moran NA. Small, smaller, smallest: the origins and evolution of ancient dual symbioses in a phloem-feeding insect. *Genome Biol Evol.* 2013;5:1675–88.
- Ankrah NYD, Chouaia B, Douglas AE. The cost of metabolic interactions in symbioses between insects and bacteria with reduced genomes. *mBio.* 2018;9:e01433-18 Wilson A, Ruby EG, editors.
- Ben-Yosef M, Pasternak Z, Jurkevitch E, Yuval B. Symbiotic bacteria enable olive flies (*Bactrocera oleae*) to exploit intractable sources of nitrogen. *J Evol Biol.* 2014;27:2695–705.
- Sannino DR, Dobson AJ, Edwards K, Angert ER, Buchon N. The *Drosophila melanogaster* gut microbiota provisions thiamine to its host. *mBio.* 2018;9:e00155-18.
- Yamada R, Deshpande SA, Bruce KD, Mak EM, Ja WW. Microbes promote amino acid harvest to rescue undernutrition in *Drosophila*. *Cell Rep.* 2015;10:865–72.
- Romano KA, Vivas EI, Amador-Noguez D, Rey FE. Intestinal microbiota composition modulates choline bioavailability from diet and accumulation of the proatherogenic metabolite trimethylamine-N-oxide. *mBio.* 2015;6:e02481-14.
- Matos RC, Schwarzer M, Gervais H, Courtin P, Joncour P, Gillet B, et al. D-Alanylation of teichoic acids contributes to *Lactobacillus plantarum*-mediated *Drosophila* growth during chronic undernutrition. *Nat Microbiol.* 2017;2:1635–47.
- Storelli G, Strigini M, Grenier T, Bozonnet L, Schwarzer M, Daniel C, et al. *Drosophila* perpetuates nutritional mutualism by promoting the fitness of its intestinal symbiont *Lactobacillus plantarum*. *Cell Metab.* 2018;27:362-377.e8.
- Storelli G, Defaye A, Erkosar B, Hols P, Royet J, Leulier F. *Lactobacillus plantarum* promotes *Drosophila* systemic growth by modulating hormonal signals through TOR-dependent nutrient sensing. *Cell Metab.* 2011;14:403–14.
- Consuegra J, Grenier T, Baa-Puyoulet P, Rahioui I, Akherraz H, Gervais H, et al. *Drosophila*-associated bacteria differentially shape the nutritional requirements of their host during juvenile growth. *PLoS Biol.* 2020;18:e3000681.
- Raza MF, Yao Z, Bai S, Cai Z, Zhang H. Tephritidae fruit fly gut microbiome diversity, function and potential for applications. *Bull Entomol Res.* 2020;110:423–37.
- Cai Z, Yao Z, Li Y, Xi Z, Bourtzis K, Zhao Z, et al. Intestinal probiotics restore the ecological fitness decline of *Bactrocera dorsalis* by irradiation. *Evol Appl.* 2018;11:1946–63.
- Wang Y, Li Z, Zhao Z. Population mixing mediates the intestinal flora composition and facilitates invasiveness in a globally invasive fruit fly. *Microbiome.* 2023;11:213.
- Ren L, Ma Y, Xie M, Lu Y, Cheng D. Rectal bacteria produce sex pheromones in the male oriental fruit fly. *Curr Biol.* 2021;31:2220-2226.e4.
- Shi Y, Wang L, Dou W, Jiang H-B, Wei D-D, Wei D, et al. Determination of instars of *Bactrocera dorsalis* (Diptera: Tephritidae). *Florida Entomologist.* 2017;100:270–5.
- Yu G, Wang L-G, Han Y, He Q-Y. clusterProfiler: an R Package for comparing biological themes among gene clusters. *OMICS.* 2012;16:284–7.
- Zhao X, Zhang X, Chen Z, Wang Z, Lu Y, Cheng D. The divergence in bacterial components associated with *Bactrocera dorsalis* across developmental stages. *Front Microbiol.* 2018;9:114.
- Behar A, Jurkevitch E, Yuval B. Bringing back the fruit into fruit fly–bacteria interactions. *Mol Ecol.* 2008;17:1375–86.
- Lauzon CR, McCombs SD, Potter SE, Peabody NC. Establishment and vertical passage of *Enterobacter (Pantoea) Agglomerans* and *Klebsiella pneumoniae* through all life stages of the mediterranean fruit fly (Diptera: Tephritidae). *Ann Entomol Soc Am.* 2009;102:85–95.
- Wang H, Jin L, Zhang H. Comparison of the diversity of the bacterial communities in the intestinal tract of adult *Bactrocera dorsalis* from three different populations: Bacterial communities in *B. dorsalis* gut. *J Appl Microbiol.* 2011;110:390–401.

45. Yao Z, Ma Q, Cai Z, Raza MF, Bai S, Wang Y, et al. Similar shift patterns in gut bacterial and fungal communities across the life stages of *Bactrocera minax* larvae from two field populations. *Front Microbiol.* 2019;10:2262.
46. Gu W, Tong P, Liu C, Wang W, Lu C, Han Y, et al. The characteristics of gut microbiota and commensal Enterobacteriaceae isolates in tree shrew (*Tupaia belangeri*). *BMC Microbiol.* 2019;19:203.
47. Zhang Q, Wang S, Zhang X, Zhang K, Liu W, Zhang R, et al. Enterobacter hormaechei in the intestines of housefly larvae promotes host growth by inhibiting harmful intestinal bacteria. *Parasites Vectors.* 2021;14:598.
48. Engel P, Moran NA. The gut microbiota of insects – diversity in structure and function. *FEMS Microbiol Rev.* 2013;37:699–735.
49. Yang Y, Liu X, Xu H, Liu Y, Lu Z. Effects of host plant and insect generation on shaping of the gut microbiota in the rice leafhopper *Cnaphalocrocis medinalis*. *Front Microbiol.* 2022;13: 824224.
50. Wang H, Jin L, Peng T, Zhang H, Chen Q, Hua Y. Identification of culturable bacteria in the intestinal tract of *Bactrocera dorsalis* from three different populations and determination of their attractive potential: Bacterial communities and function in *B. dorsalis* gut. *Pest Manag Sci.* 2014;70:80–7.
51. Wang H, Jin L, Zhang H. Comparison of the diversity of the bacterial communities in the intestinal tract of adult *Bactrocera dorsalis* from three different populations. *J Appl Microbiol.* 2011;110:1390–401.
52. Shin SC, Kim S-H, You H, Kim B, Kim AC, Lee K-A, et al. *Drosophila* microbiome modulates host developmental and metabolic homeostasis via insulin signaling. *Science.* 2011;334:670–4.
53. Martinson VG, Strand MR. Diet–microbiota interactions alter mosquito development. *Front Microbiol.* 2021;12:650743.
54. Consuegra J, Grenier T, Akherraz H, Rahioui I, Gervais H, Da Silva P, et al. Metabolic cooperation among commensal bacteria supports *Drosophila* juvenile growth under nutritional stress. *iScience.* 2020;23:101232.
55. Zheng H, Powell JE, Steele MI, Dietrich C, Moran NA. Honeybee gut microbiota promotes host weight gain via bacterial metabolism and hormonal signaling. *Proc Natl Acad Sci USA.* 2017;114:4775–80.
56. Behar A, Yuval B, Jurkevitch E. Enterobacteria-mediated nitrogen fixation in natural populations of the fruit fly *Ceratitis capitata*. *Mol Ecol.* 2005;14:2637–43.
57. Huang S-W, Zhang H-Y, Marshall S, Jackson TA. The scarab gut: A potential bioreactor for bio-fuel production. *Insect Science.* 2010;17:175–83.
58. Huang S, Sheng P, Zhang H. Isolation and identification of cellulolytic bacteria from the gut of *Holotrichia parallela* Larvae (Coleoptera: Scarabaeidae). *Int J Mol Sci.* 2012;13:2563–77.
59. Sheng P, Huang S, Wang Q, Wang A, Zhang H. Isolation, screening, and optimization of the fermentation conditions of highly cellulolytic bacteria from the hindgut of *Holotrichia parallela* Larvae (Coleoptera: Scarabaeidae). *Appl Biochem Biotechnol.* 2012;167:270–84.
60. Sheng P, Xu J, Saccone G, Li K, Zhang H. Discovery and characterization of endo-xylanase and β -xylosidase from a highly xylanolytic bacterium in the hindgut of *Holotrichia parallela* larvae. *J Mol Catal B Enzym.* 2014;105:33–40.
61. Guo Q, Yao Z, Cai Z, Bai S, Zhang H. Gut fungal community and its probiotic effect on *Bactrocera dorsalis*. *Insect Sci.* 2022;29:1145–58.
62. Purdy AE, Watnick PI. Spatially selective colonization of the arthropod intestine through activation of *Vibrio cholerae* biofilm formation. *Proc Natl Acad Sci U S A.* 2011;108:19737.
63. Dodge R, Jones EW, Zhu H, Obadia B, Martinez DJ, Wang C, et al. A symbiotic physical niche in *Drosophila melanogaster* regulates stable association of a multi-species gut microbiota. *Nat Commun.* 2023;14:1557.
64. Barnard K, Jeanrenaud ACSN, Brooke BD, Oliver SV. The contribution of gut bacteria to insecticide resistance and the life histories of the major malaria vector *Anopheles arabiensis* (Diptera: Culicidae). *Sci Rep.* 2019;9:9117.
65. Kim JK, Kwon JY, Kim SK, Han SH, Won YJ, Lee JH, et al. Purine biosynthesis, biofilm formation, and persistence of an insect-microbe gut symbiosis. *Appl Environ Microbiol.* 2014;80:4374–82 Lovell CR, editor.
66. Abraham NM, Liu L, Jutras BL, Yadav AK, Narasimhan S, Gopalakrishnan V, et al. Pathogen-mediated manipulation of arthropod microbiota to promote infection. *Proc Natl Acad Sci U S A.* 2017;114:E781–90.
67. Jiang Y, Gao H, Wang L, Hu W, Wang G, Wang S. Quorum sensing-activated phenylalanine metabolism drives OMV biogenesis to enhance mosquito commensal colonization resistance to *Plasmodium*. *Cell Host Microbe.* 2023;31:1655–1667.e6.
68. Douglas AE. The B vitamin nutrition of insects: the contributions of diet, microbiome and horizontally acquired genes. *Curr Opin Insect Sci.* 2017;23:65–9.
69. Wong ACN, Dobson AJ, Douglas AE. Gut microbiota dictates the metabolic response of *Drosophila* to diet. *J Exp Biol.* 2014;217:1894.
70. Wang Y, Eum JH, Harrison RE, Valzania L, Yang X, Johnson JA, et al. Riboflavin instability is a key factor underlying the requirement of a gut microbiota for mosquito development. *Proc Natl Acad Sci USA.* 2021;118:e2101080118.
71. Serrato-Salas J, Gendrin M. Involvement of microbiota in insect physiology: focus on B vitamins. *mBio.* 2022;14:02225–22.
72. Michalkova V, Benoit JB, Weiss BL, Attardo GM, Aksoy S. Vitamin B6 generated by obligate symbionts is critical for maintaining proline homeostasis and fecundity in tsetse flies. *Appl Environ Microbiol.* 2014;80:5844–53.

Publisher's Note

Springer Nature remains neutral with regard to jurisdictional claims in published maps and institutional affiliations.